Multiplicity of transmission coefficients in photonic crystal and split ring resonator waveguides with Kerr nonlinear impurities

Buddhi Rai[1] and Arthur R. McGurn[2]

[1]*Department of Science Technology Engineering and Mathematics, University of Hawaii Maui College, 310 W Kaahumanu Ave, Kahului, Hawaii 96732-1617, USA*

[2]*Department of Physics, Western Michigan University, 1903 W Michigan Ave, Kalamazoo, Michigan 49008-5252, USA*

(Received 20 May 2014; revised manuscript received 8 January 2015; published 19 February 2015)

Photonic crystal and split ring resonator (SRR) metamaterial waveguides with Kerr nonlinear dielectric impurities are studied. The transmission coefficients for two guided modes of different frequencies scattering from the Kerr impurities are computed. The systems are shown to exhibit multiple transmission coefficient solutions arising from the Kerr nonlinearity. Multiple transmission coefficients occur when different input intensities into a waveguide result in the same transmitted output intensities past its nonlinear impurities. (In the case of a single incident guided mode the multiplicity of transmission coefficients is known as optical bistability.) The analytical conditions under which the transmission coefficients are single and multiple valued are determined, and specific examples of both single and multiple valued transmission coefficient scattering are presented. Both photonic crystal and split ring resonator systems are studied as the Kerr nonlinearity enters the photonic crystal and SRR systems in different ways. This allows for an interesting comparison of the differences in behaviors of these two types of system which are described by distinctly different mathematical structures. Both the photonic crystal and SRR models used in the calculations are based on a difference equation approach to the system dynamics. The difference equation approach has been extensively employed in previous papers to model the basic properties of these systems. The paper is a continuation of work on the optical bistability of single guided modes interacting with Kerr impurities in photonic crystals originally considered by McGurn [Chaos **13**, 754 (2003)] and work on the resonant scattering from Kerr impurities in photonic crystal waveguides considered by McGurn [J. Phys.: Condens. Matter **16**, S5243 (2004)]. It generalizes this work making the extension to the more complex interaction of two guided modes at different frequencies. It extends the two guided mode treatment by McGurn [Organ. Electron. **8**, 227 (2007)] which was limited to a special case of one of the photonic crystal systems considered here.

DOI: 10.1103/PhysRevB.91.085113 PACS number(s): 78.67.Pt, 81.05.Xj, 42.65.−k, 05.45.−a

I. INTRODUCTION

Photonic crystals [1–8], split ring resonator (SRR) metamaterials [9–20], and their applications in waveguide designs have been of considerable current interest. Great efforts have been applied in determining the physical principles behind the effective operation of these systems and in the extensions of their applications. Most of the recent focus has been on linear dynamical systems, but nonlinear properties are important as many device applications such as optical switching require nonlinear dynamics [5,6,9,14–33]. Nonlinearity opens the possibility for new features in these systems as it allows for the interaction of the modes of the linear limit of the system and increases the number and types of solutions over those of linear systems [9,21–25,29–33]. These are necessary properties for device designs that do more than simply conduct energy or signals. In this paper some basic properties related to the nonlinear dynamics of simple waveguides in photonic crystal and split ring resonator (SRR) systems are investigated [1–9,14–24,29,30,32,34–36].

In particular, the focus is on waveguides interacting with nonlinear dielectric impurities and how these impurities modify the elastic scattering of the guided modes [33–38]. In one case a nonlinear impurity introduced as a replacement site within the waveguide channel is treated, and in a second case a nonlinear impurity introduced next to but outside the waveguide channel is treated. Aside from renormalizing the impurity scattering from the linear dielectric limit of these systems, the nonlinearity allows for the guided modes to interact with one another and to exhibit multiple transmission solutions for modes incident on the impurities [39,40]. In the case of a single guided mode in the system the presence of multiple transmission solutions is known as optical bistability. In this paper we will consider the more general case of two guided modes of different frequencies traveling and interacting in the system. The multiple mode problems for two guided waves lead to more complex transmission behaviors in the systems than that found in the single mode problem. This multiplicity of the transmission coefficients is a feature which is introduced by the nonlinearity, and understanding the conditions for its occurrence is the focus of this paper.

Photonic crystal waveguides have been extensively studied using both numerical and analytical methods [1–9]. A common method of study is based on numerical computer simulation techniques [1–3,21]. These have led to important and well known engineering results for impurities, waveguide branchings, and couplings of general waveguide systems. Analytical methods can also be applied to some systems, giving insights into the quantitative and qualitative properties of waveguides and configurations of waveguides [5–10,21–24,33–38]. In this paper we focus on the later analytic approach based on difference equations. The basis of the approach is a set of difference equations which are developed in a type of coupled resonator treatment [5,6,21–24,29,30,33–35,41]. The difference equation approach [41] has been applied in a variety of discussions of the properties of nonlinear systems

for the transmission of guided modes through impurities and arrays of impurities and for waveguide branchings [5,6,21–24,29,30,33–35,41]. Its analytic nature leads to analytical forms that, in the present considerations of the impurity waveguide systems, give a complete determination of the transmission solutions in terms of parameters which can be estimated for any experimental realization of waveguides.

Another nanosystem with a difference equation approach is an SRR metamaterial. SRR metamaterials are of interested as they allow for the design of artificial materials with engineered optical properties not found in natural, nonengineered, materials [9,14–16,32,33]. This has given rise to technological and device applications, e.g., negative refractive index materials [9–12,42–44], superlenses [13], cloaking devices [42], and relativistically modeled materials [45,46]. The development of the linear and nonlinear difference equations for these systems has been given in a variety of papers and is outlined later for the nonlinear system [14–16,32,33]. Studies of these systems have focused on the dynamical properties of both linear and nonlinear SRR materials, with much work directed to understanding the nature of the modes occurring in various systems and their classification. In this paper we extend this work with a focus on one-dimensional waveguide chains of SRR interacting with optically nonlinear media.

For both the photonic crystal and SRR systems our emphasis is on multiple transmission coefficients found in the scattering of multiple guided modes from the nonlinear impurity sites. By multiple transmission coefficients we mean that there are a number of different inputs of incident guided modes that result in the same output guided mode past the scattering impurity. Similar types of discussions in other contexts have been made in the treatment of the optical bistability of the scattering of a single frequency of light from a Kerr nonlinear dielectric slab [31,39,40]. Kerr nonlinearity enters the photonic crystal and SRR systems in different ways and this allows for an interesting comparison between the different mathematics and solutions of these systems [33].

The focus of the paper is to extend the work in Refs. [34,35,47] to develop general analytical criterion, for the nonlinear impurity scattering of guided modes of single and multiple frequencies, that indicate the appearance of multiple transmission solutions in photonic crystal systems. These considerations are then continued to make similar considerations for the SRR metamaterials. In order to simplify the discussions in the present paper, though the general formulation of the two guided mode scattering problem is treated, results are only presented for modes with closely spaced frequencies. This limits the number of cases discussed while still considering a set which have interesting properties and technological potential. The order of the paper is as follows: In Sec. II the models of the waveguides with impurities are presented. The algebraic solutions of the models are presented in Sec. III along with the conditions for multiple transmission coefficients. In Sec. IV the solutions are discussed and illustrated for some simple cases. In Sec. V are the conclusions. It is hoped that our results will make a contribution to recent studies that have focused on optical bistability in nanophotonic systems [48–52].

II. MODELS

The scattering of two guided modes by nonlinear dielectric impurities is studied in nanoscience waveguides. Both in-channel and off-channel impurities are considered, and the impurities are composed of Kerr nonlinear media so that the guided modes interact with themselves and with one another. This introduces an additional complication from the scattering due to linear dielectric impurities.

In the first study a photonic crystal waveguide modeled in a difference equation approach is considered [29,30,35,41]. This approach has been used previously on other systems with a focus on different properties and geometries [22–24,29,30,34–36,41,47]. The second system studied is a split ring resonator (SRR) metamaterial, also formulated in a difference equation approach [9,14–16,32,33]. In the treatment of the SRR metamaterial the system is modeled as a chain of inductor-capacitor (LC) resonator circuits that are coupled to one another through mutual induction. It is a simplification of more general three-dimensional models of SRR metamaterials.

Aside from their nanoscience applications, the two systems are of interest because the dielectric nonlinearity enters the difference equations of the photonic crystal and metamaterials differently [33]. This allows an interesting comparison of the dynamical properties of these two nonlinear models.

In the approximation of a Kerr nonlinear dielectric media the index of refraction is a function of the intensity of the applied electric field, and various inelastic frequency mixing effects leading to the generation of higher harmonics are ignored [26–28,39,40]. This is known as the rotating wave approximation (RWA). The field dependence of the dielectric properties of the Kerr media allows two modes of different frequency to modulate each other's transmission through the system. In addition, each mode self-modulates its own transmission through the system. In the discussions later, the model of the photonic crystal system is first presented. This is followed by the presentation of the model of the metamaterial.

A. Photonic crystal

The in-channel scattering geometry is shown in the schematic of Fig. 1(a). Here we consider a two-dimensional photonic crystal composed of infinite parallel axis dielectric

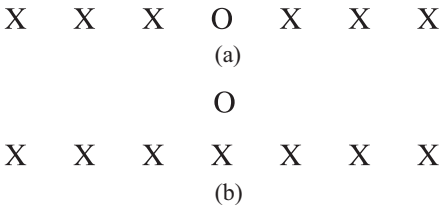

FIG. 1. Schematic plot of a one-dimensional waveguide of linear media sites (denoted X) interacting with an impurity site of nonlinear media (denoted 0) for: (a) the impurity formed as a replacement site within the waveguide channel, and (b) the impurity formed by site replacement off the waveguide channel. Only the sites of the waveguide and impurities are shown. For the photonic crystal studies, the waveguide and impurities are formed by cylinder replacement in a square lattice photonic crystal, with the waveguide channel along the x axis of the square lattice of the photonic crystal.

cylinders of radii R. The cylinders are arranged on a square lattice of lattice constant $a > 2R$ in the plane perpendicular to the common axis of the cylinders. A waveguide is formed by cylinder replacement of a single row of cylinders along the x axis with cylinders containing a change in dielectric permittivity $\delta\varepsilon_l$ in a region of radius $r \ll R$ about the axis of each replacement cylinder. An in-channel impurity is formed for one of the cylinders in the waveguide channel by taking the change in dielectric of that cylinder to be in the form of a Kerr nonlinear optical medium. For a single frequency mode the permittivity change due to the presence of Kerr medium is of the form $\delta\varepsilon(|E|^2) = \delta\varepsilon(1 + \lambda|E|^2)$, where λ characterizes the nonlinearity [29,30]. In the presence of two different frequency modes labeled by i, $j = 1, 2$ with $i \neq j$, the change in the dielectric permittivities due to the presence of the added linear medium become $\delta\varepsilon_l^i$ and the change in the dielectric permittivities due to the presence of the added Kerr medium permittivity is $\delta\varepsilon^i(|E_i|^2, |E_j|^2) = \delta\varepsilon^i(1 + \lambda_{ii}|E_i|^2 + \lambda_{ij}|E_j|^2)$ [35]. Here λ_{ii} and λ_{ij}, respectively, characterize the self-interaction of the modes and the interaction between the modes. For $\lambda_{ij} = 0$ the dielectric form reduces to that of a single i frequency mode in the system.

Within the coupled resonator approach, the difference equations for the in-channel system are given by [29,30,35,41,47]

$$E_n^i = g_l^i \left[\alpha_i E_n^i + \beta_i \left(E_{n+1}^i + E_{n-1}^i\right)\right], \tag{1a}$$

for $n > 1$ or $n < -1$, and

$$E_0^i = g^i\alpha_i\left[1 + \lambda_{ii}\left|E_0^i\right|^2 + \lambda_{ij}\left|E_0^j\right|^2\right]E_0^i + g_l^i\beta_i\left(E_1^i + E_{-1}^i\right), \tag{1b}$$

$$E_{\pm1}^i = g_l^i\left(\alpha_i E_{\pm1}^i + \beta_i E_{\pm2}^i\right) + g^i\beta_i\left[1 + \lambda_{ii}\left|E_0^i\right|^2 + \lambda_{ij}\left|E_0^j\right|^2\right]E_0^i. \tag{1c}$$

Here $i, j = 1,2$ with $j \neq i$ label the two different frequency modes sent down the waveguide, and E_n^i is the electric field at the center of the nth replacement cylinder for the frequency mode labeled i. The coefficients $g_l^i = \delta\varepsilon_l^i$ and $g^i = \delta\varepsilon^i$; and the on-site and nearest neighbor couplings α_i and β_i are related to the on-site site and nearest neighbor site Green's functions of the bulk photonic crystal. At each guided mode frequency the ratio $|\frac{\beta_i}{\alpha_i}| \ll 1$ has been shown elsewhere to exhibit a roughly exponential decay with the separation between sites, and the ratio is easily adjusted by changing the separation between neighboring sites chosen to form the waveguide channel [47]. Consequently, the approach in Eq. (1) is for a system with weak nearest neighbor couplings, and further neighbor couplings are not and need not be treated.

The off-channel scattering geometry is given in the schematic of Fig. 1(b). The representation is of a waveguide channel along the x axis in a two-dimensional photonic crystal with an off-channel Kerr nonlinear impurity set one lattice constant away from the waveguide channel along the y axis. Here one of the off-channel photonic crystal cylinders is replaced by a channel cylinder containing Kerr nonlinear optical media.

The difference equations for this system are given by [29,30,35,41,47]

$$E_n^i = g_l^i \left[\alpha_i E_n^i + \beta_i \left(E_{n+1}^i + E_{n-1}^i\right)\right], \tag{2a}$$

for $n \geqslant 1$ or $n \leqslant -1$, and where s labels the off-channel site

$$E_0^i = g_l^i \left[\alpha_i E_0^i + \beta_i \left(E_1^i + E_{-1}^i\right)\right] + g^i\beta_i\left[1 + \lambda_{ii}\left|E_s^i\right|^2 + \lambda_{ij}\left|E_s^j\right|^2\right]E_s^i, \tag{2b}$$

$$E_s^i = g^i\alpha_i\left[1 + \lambda_{ii}\left|E_s^i\right|^2 + \lambda_{ij}\left|E_s^j\right|^2\right]E_s^i + g_l^i\beta_i E_0^i. \tag{2c}$$

Here $i, j = 1,2$, with $j \neq i$, label the two different frequency modes sent down the waveguide, and the parameters in Eqs. (2) are the same as those in Eqs. (1).

Solutions to Eqs. (1) and (2) are obtained algebraically for scattering boundary conditions of the form [22–24]

$$E_n^i = t_i e^{ik_i n}, \tag{3a}$$

with real t_i for $n \geqslant 1$ and

$$E_n^i = u_i e^{ik_i n} + v_i e^{-ik_i n}, \tag{3b}$$

for $n \leqslant -1$. With these boundary conditions the sums of the transmission and reflection coefficients of each mode are unity.

B. Metamaterial

The system consists of self-inductive metal rings that are split with a capacitive gap of width d containing dielectric material. These are the SRR. The dielectric material in the gaps is optically linear in the waveguide channel and optically Kerr nonlinear in the impurities. Each SRR forms an LRC circuit with a time-varying current and capacitive charge. The metamaterial is composed as a linear chain of SRR basis elements on a one-dimensional Bravais lattice of lattice constant a. The SRR along the chain interact with one another by weak nearest neighbor mutual inductive couplings [14–16,32,33].

For a single frequency mode the linear medium permittivity of the gap material is $\varepsilon_0\varepsilon_l$, and in the RWA the Kerr dielectric permittivity of the gap material is $\varepsilon(|E|^2) = \varepsilon_0(\varepsilon_l + \alpha\frac{|E|^2}{E_c^2})$ for E_c a characteristic (large) electric field, and where $\alpha = \pm1$ indicates the self-focusing or self-defocusing properties of the Kerr medium [32,33]. In the presence of two frequencies labeled by i, $j = 1, 2$, with $i \neq j$, the permittivities of the linear medium become $\varepsilon_0\varepsilon_l^i$ and the Kerr medium permittivity in the RWA is $\varepsilon^i(|E_i|^2, |E_j|^2) = \varepsilon_0(\varepsilon_l^i + \alpha\frac{|E_i|^2}{(E_c^{ii})^2} + \alpha\frac{|E_j|^2}{(E_c^{ij})^2})$, where E_c^{ii} and E_c^{ij} are characteristic electric fields at the two different frequencies [35].

The problem of the in-channel Kerr nonlinear dielectric impurity in a waveguide chain of SRR is represented schematically in Fig. 1(a) [14–16,32,33]. The difference equations describing the dynamics of the system are [32,33]

$$-\omega_i^2\left[q_n^i + \lambda_i\left(q_{n+1}^i + q_{n-1}^i\right)\right] + q_n^i = 0, \tag{4a}$$

for $n \geqslant 1$ or $n \leqslant -1$, and

$$-\omega_i^2\left[q_0^i + \lambda_i\left(q_1^i + q_{-1}^i\right)\right] + q_0^i - \left[\left(\frac{3\alpha}{\varepsilon_l^i} r_{ii}\right)\left|q_0^i\right|^2 + \left(\frac{2\alpha}{\varepsilon_l^i} r_{ij}\right)\left|q_0^j\right|^2\right] q_0^i = 0. \quad (4b)$$

Here $i, j = 1,2$, with $j \neq i$, label the two different frequency modes sent down the waveguide so that $q_n^i = \frac{Q_n^i}{Q_c}$, where Q_n^i is the charge on the nth SRR of the ith mode and Q_c is a normalizing constant which is defined later. The couplings $\lambda_i = \frac{M_i}{L_i}$, where M_i is the mutual inductive couplings between nearest neighbor SRR and L_i is the SRR self-inductance of the ith mode. (Note that, following previous treatments, in the systems studied further than nearest neighbor mutual inductive couplings are assumed to be small. A detailed discussion of this approximation is given in Refs. [32,33].) Defining a characteristic linear gap capacitance $C = (C_l^1 + C_l^2)/2$, where C_l^i is the linear gap capacitance (i.e., $\lambda_{ii} = \lambda_{ij} = 0$) of the ith mode and a characteristic SRR gap potential $U_c = (E_c^1 + E_c^2)d/2$, the normalizing charge $Q_c = CU_c$ is obtained from the capacitor formula. In terms of these $r_{ii} = (\frac{Q_c}{C_l^i U_c^{ii}})^2$ and $r_{ij} = (\frac{Q_c}{C_l^j U_c^{ij}})^2$, where $U_c^{ii} = E_c^{ii} d$ and $U_c^{ij} = E_c^{ij} d$ are characteristic gap potentials giving the strength of the nonlinear interactions at frequencies i and j. Finally, the frequency related coefficients are defined as $\omega_i^2 = \Omega_i^2 \frac{L_i C_i}{LC}$, where Ω_i is the frequency of the ith mode in units of $\frac{1}{\sqrt{LC}}$ and where $L = (L_1 + L_2)/2$ is a characteristic self-inductance of the SRR.

The off-channel impurity in the SRR waveguide is shown schematically in Fig. 1(b). The difference equations describing the waveguide are given by [32,33]

$$-\omega_i^2\left[q_n^i + \lambda_i\left(q_{n+1}^i + q_{n-1}^i\right)\right] + q_n^i = 0, \quad (5a)$$

for $n \geqslant 1$ or $n \leqslant -1$,

$$-\omega_i^2\left[q_0^i + \lambda_i\left(q_1^i + q_{-1}^i\right)\right] + q_0^i - \omega_i^2 \lambda_i' q_s^i = 0, \quad (5b)$$

and

$$-\omega_i^2\left[q_s^i + \lambda'_i q_0^i\right] + q_s^i - \left[\left(\frac{3\alpha}{\varepsilon_l^i} r_{ii}\right)\left|q_s^i\right|^2 + \left(\frac{2\alpha}{\varepsilon_l^i} r_{ij}\right)\left|q_s^j\right|^2\right] q_s^i = 0, \quad (5c)$$

for the 0 site and the off-channel site labeled s. In these equations, $\lambda_i' = \frac{M'_i}{L_i}$ allows for a difference in the off-channel mutual inductance, and the notation is otherwise the same as that in Eqs. (4).

Solutions to Eqs. (4) and (5) are obtained algebraically for boundary conditions in the form [22–24]

$$q_n^i = t_i e^{ik_i n}, \quad (6a)$$

with real t_i for $n \geqslant 1$ and

$$q_n^i = u_i e^{ik_i n} + v_i e^{-ik_i n}, \quad (6b)$$

for $n \leqslant -1$. The transmission and reflections coefficients of each frequency mode sum to unity for these boundary conditions.

III. SOLUTIONS

In this section solutions of the nonlinear scattering problems are given for the photonic crystal systems in Eqs. (1) and (2) and the metamaterials systems in Eqs. (4) and (5). This is followed by discussions of the origins and nature of the multiple solution properties of these systems.

A. Photonic crystals

The photonic crystal in-channel and off-channel nonlinear impurity problems for two different interacting guided frequency modes are solved algebraically. The solutions are obtained for the boundary conditions given in Eqs. (3).

In both problems two scattering modes (labeled $i = 1, 2$) with dispersion relations

$$1 = g_l^i\left[\alpha_i + 2\beta_i \cos k_i\right] \quad (7)$$

propagate in the linear media waveguide and are incident on impurity sites of nonlinear optical media. The scattering solutions are written in terms of the normalized variables $\tilde{u}_i = \frac{u_i}{t_i}$, $\tilde{v}_i = \frac{v_i}{t_i}$, $\tilde{S}_i = \frac{S_i}{t_i}$, $\gamma_{ii} = \lambda_{ii} t_i^2$, and $\gamma_{ij} = \lambda_{ij} t_j^2$, where $i = 1, 2$. (Notice that in this notation the couplings γ_{ii} and γ_{ij} depend on the Kerr parameters of the nonlinear dielectric and on the amplitudes of the transmitted guided modes.) The two incident modes interact with themselves and one another through the nonlinearity of the impurity sites.

For both in-channel and off-channel systems

$$\tilde{u}_i = 1 - \tilde{v}_i, \quad (8)$$

where for the in-channel problem

$$\tilde{v}_i = \frac{1}{2i \sin k_i} \frac{\tilde{S}_i - 1}{g_l^i \beta_i} \quad (9)$$

and for the off-channel problem

$$\tilde{v}_i = \frac{1}{2i \sin k_i} \frac{g_l^i \beta_i - \tilde{S}_i}{\alpha_i g_l^i}. \quad (10)$$

The variables $\tilde{S}_i$ in Eq. (9) for the in-channel problem are determined as solutions of the nonlinear equations

$$\gamma_{ii}|\tilde{S}_i|^2 \tilde{S}_i + (1 + \gamma_{ij}|\tilde{S}_j|^2)\tilde{S}_i - \frac{g_l^i}{g^i} = 0, \quad (11)$$

for $i = 1, 2$, and the variables $\tilde{S}_i$ in Eq. (10) for the off-channel problem are solutions of the nonlinear equations

$$\gamma_{ii}|\tilde{S}_i|^2 \tilde{S}_i + \left(\gamma_{ij}|\tilde{S}_j|^2 + 1 - \frac{1}{g^i \alpha_i}\right)\tilde{S}_i + \frac{g_l^i \beta_i}{g^i \alpha_i} = 0, \quad (12)$$

for $i = 1, 2$. The effects of nonlinearity in the two problems enter through the nonlinear Eqs. (11) and (12). Consequently, the key to explaining the behaviors of the scattering interaction in these systems is in understanding the solutions of Eqs. (11) and (12). This will be the focus of the discussions in the following.

In the considerations of each of the two scattering problems, the transmission coefficients of the two frequency modes are obtained by solving Eqs. (7) through (12) for $\tilde{u}_i = \frac{u_i}{t_i}$, $\tilde{v}_i = \frac{v_i}{t_i}$, and $\tilde{S}_i = \frac{S_i}{t_i}$. Specifically, for the in-channel (off-channel) problem the solutions of the $\tilde{S}_i$'s in Eq. (11) [Eq. (12)] are

determined. Once these $\tilde{S}_i$ are obtained, they are used in Eqs. (8) and (9) to determine $(\tilde{u}_i, \tilde{v}_i)$ of the in-channel problem or in Eqs. (8) and (10) to determine $(\tilde{u}_i, \tilde{v}_i)$ of the off-channel, respectively. The transmission coefficients are then given by $T_i = |\frac{1}{\tilde{u}_i}|^2$ and the reflection coefficients by $R_i = |\frac{\tilde{v}_i}{\tilde{u}_i}|^2$. For both the in-channel and off-channel solutions $R_i + T_i = 1$ is separately satisfied for each of the two incident frequency modes.

B. Metamaterials

The metamaterial in-channel and off-channel nonlinear impurity problems for two different interacting guided frequency modes are solved algebraically. The solutions are generated for the boundary conditions in Eqs. (6).

For both the in-channel and off-channel problems the incident guided modes (labeled $i = 1, 2$) have dispersion relations

$$\omega_i^2 = \frac{1}{1 + 2\lambda_i \cos k_i}, \tag{13}$$

for propagation in the linear media waveguides, and in each problem the modes interact with themselves and each other at the Kerr nonlinear impurities. The scattering solutions are written in terms of the normalized variables $\tilde{u}_i = \frac{u_i}{t_i}$, $\tilde{v}_i = \frac{v_i}{t_i}$, $\gamma_{ii} = \frac{3\alpha}{\varepsilon_i^i} r_{ii} t_i^2$, and $\gamma_{ij} = \frac{2\alpha}{\varepsilon_i^i} r_{ij} t_j^2$, where $i = 1, 2$, and as with the photonic crystal problems the coupling coefficients depend on the amplitudes of the transmitted guided modes. For both the in-channel and off-channel systems

$$\tilde{v}_i = 1 - \tilde{u}_i, \tag{14}$$

where for the in-channel problem

$$\tilde{u}_i = 1 + \frac{1}{2i \sin k_i} \left[\frac{\gamma_{ii} + \gamma_{ij}}{\omega_i^2 \lambda_i} \right] \tag{15}$$

and for the off-channel problem

$$\tilde{v}_i = -\frac{1}{2i \sin k_i} \frac{\lambda_i{}'}{\lambda_i} \tilde{S}_i. \tag{16}$$

The variables $\tilde{S}_i$ in Eq. (16) for the off-channel problem are determined as solutions of the nonlinear equations

$$|\tilde{S}_i|^2 \tilde{S}_i + \frac{\omega_i^2 - 1 + \gamma_{ij} |\tilde{S}_j|^2}{\gamma_{ii}} \tilde{S}_i + \frac{\omega_i^2 \lambda_i{}'}{\gamma_{ii}} = 0. \tag{17}$$

Note that only the off-channel problem has a multiplicity of solutions arising from the nonlinearity of Eq. (17), and the solution of the in-channel problem given by Eqs. (14) and (15) does not exhibit a multiplicity of solutions. For the in-channel problem the nonlinearity only renormalizes the single solution for the transmission and reflection coefficients, and, consequently, the in-channel problem will not be discussed further.

The transmission coefficients are obtained by Eqs. (14) through (17) for $\tilde{u}_i = \frac{u_i}{t_i}$, $\tilde{v}_i = \frac{v_i}{t_i}$, and in the case of the off-channel problem for $\tilde{S}_i = \frac{S_i}{t_i}$. For the off-channel problem the solutions of the $\tilde{S}_i$'s are determined from Eq. (17), and these are used to obtain $(\tilde{u}_i, \tilde{v}_i)$ from Eqs. (14) and (16). In both the off- and in-channel problems the transmission coefficients are given by $T_i = |\frac{1}{\tilde{u}_i}|^2$ and the reflection coefficients are given by $R_i = |\frac{\tilde{v}_i}{\tilde{u}_i}|^2$ so that for each guide frequency mode $R_i + T_i = 1$.

We now discuss the multiple solution nature of the transmission coefficients found in both the photonic crystal and metamaterial systems.

C. Solutions of the set of two nonlinear equations

The multiple solution transmission characteristics of the photonic crystal waveguide and the SRR metamaterial are discussed for representative solutions of the two nonlinear systems. What is meant by optical multiple solutions in the case of a single frequency mode is that, for a fixed parametrization of the difference equations and a fixed specification of the output intensity in the waveguide channel, the solutions for the input intensity of the scattered wave display multiple values giving the same output intensity. What is meant by optical multiple solutions for two frequencies modes is that for a fixed parametrization of the difference equations and a fixed specification of the output intensities in the waveguide channel, the solutions for the input intensities of the scattered waves display multiple values giving the same output intensities.

The multiplicity of transmission coefficients for the photonic crystal and metamaterial scattering comes from the multiple solutions of the $\tilde{S}_i$'s obtained from each of Eqs. (11), (12), or (17). These nonlinear equations for the $\tilde{S}_i$'s do not involve the other $\tilde{u}_i = \frac{u_i}{t_i}$, $\tilde{v}_i = \frac{v_i}{t_i}$ variables that are obtained as linear functions of the $\tilde{S}_i$'s solutions. Consequently, in the following the focus is on understanding the multiple solutions of the $\tilde{S}_i$'s obtained from Eqs. (11), (12), or (17). In addition, as these equations all have the same general form it is only necessary to give discussions about equations of that general form.

The sets of two nonlinear equations which define the multiple solution properties of the scattering problems are of a common form given by

$$a_1 |x|^2 x + (b_1 + c_1 |y|^2) x - d_1 = 0, \tag{18a}$$

$$a_2 |y|^2 y + (b_2 + c_2 |x|^2) y - d_2 = 0. \tag{18b}$$

Here $(x, y) = (\tilde{S}_i, \tilde{S}_j)$ and the coefficients a_i, b_i, c_i, d_i are obtained from Eqs. (11), (12), or (17). The coefficients a_i, b_i, c_i, d_i are real so that the solution sets $\{(x, y)\}$ of Eqs. (18) must be real. The solutions of Eqs. (18) are then given as the real solutions of the polynomial system

$$a_1 x^3 + (b_1 + c_1 y^2) x - d_1 = 0, \tag{19a}$$

$$a_2 y^3 + (b_2 + c_2 x^2) y - d_2 = 0, \tag{19b}$$

and the focus will be on this system. Even though Eqs. (19a) and (19b) are coupled in both x and y, they have the underlying basic form of cubic equations in x and y, respectively. The multiple solution properties of the systems are then based on those of the solutions of cubic polynomials, and these properties are now reviewed.

The regions in which each of Eqs. (19a) and (19b) exhibit single solution sets in some cases are determined by considering the solutions of cubic equations. Specifically, for a cubic polynomial of the form

$$x^3 + ax - b = 0, \tag{20a}$$

TABLE I. Conditions under which single-valued solutions are obtained for in- and off-channel photonic crystal and off-channel metamaterial impurities. Here $i, j = 1, 2$ and $i \neq j$.

In-channel photonic crystals	$\gamma_{ii} = \gamma_{jj}, \gamma_{ij} = \gamma_{ji}$	$\gamma_{ii} + \gamma_{ij} < -\frac{4}{27}\left(\frac{g^i}{g^i_l}\right)^2$ or $\gamma_{ii} + \gamma_{ij} > 0$
Off-channel photonic crystals	$\gamma_{ii} = \gamma_{jj}, \gamma_{ij} = \gamma_{ji}$ and $D_i = 1 - \frac{g^i_l}{g^i}\left[1 + 2\frac{\beta_i}{\alpha_i}\cos k_i\right] > 0$	$\gamma_{ii} + \gamma_{ij} < -\frac{4}{27}\left(\frac{g^i\alpha_i}{g^i_l\beta_i}\right)^2 {D_i}^3$ or $\gamma_{ii} + \gamma_{ij} > 0$
Off-channel photonic crystals	$\gamma_{ii} = \gamma_{jj}, \gamma_{ij} = \gamma_{ji}$ and $D_i = 1 - \frac{g^i_l}{g^i}\left[1 + 2\frac{\beta_i}{\alpha_i}\cos k_i\right] < 0$	$\gamma_{ii} + \gamma_{ij} > -\frac{4}{27}\left(\frac{g^i\alpha_i}{g^i_l\beta_i}\right)^2 {D_i}^3$ or $\gamma_{ii} + \gamma_{ij} < 0$
Off-channel metamaterials	$\gamma_{ii} = \gamma_{jj}, \gamma_{ij} = \gamma_{ji}$ and $D_i = (\omega_l^2 - 1) = -2\omega_i^2\lambda_i \cos k_i > 0$	$\gamma_{ii} + \gamma_{ij} < -\frac{4}{27}(\omega_i^2\lambda'_i)^{-2}{D_i}^3$ or $\gamma_{ii} + \gamma_{ij} > 0$
Off-channel metamaterials	$\gamma_{ii} = \gamma_{jj}, \gamma_{ij} = \gamma_{ji}$ and $D_i = (\omega_l^2 - 1) = -2\omega_i^2\lambda_i \cos k_i < 0$	$\gamma_{ii} + \gamma_{ij} > -\frac{4}{27}(\omega_i^2\lambda'_i)^{-2}{D_i}^3$ or $\gamma_{ii} + \gamma_{ij} < 0$

where a, b are real, the polynomial has one real solution for x under the condition that [53]

$$D = \frac{1}{27}a^3 + \frac{1}{4}b^2 > 0. \tag{20b}$$

In the following it is shown that under appropriate conditions on the parameters a_i and b_i Eq. (20b) must be separately satisfied by each of Eqs. (19a) (considered as a cubic in x) and (19b) (considered as a cubic in y) in order that they exhibit a unique (x, y) solution. For these cases, the simultaneous satisfaction of these conditions by the solutions of both equations provides a bound on the regions of single solutions for the transmission coefficient of the scattering problems. Some examples of this are considered later.

1. Case illustrations

The parameter space of Eqs. (19) is large for general considerations of scattering problems involving two guided modes. However, some special cases of interest for physical and technological applications can be drawn upon as a focus of considerations. These give indications of new behaviors, not observed in the optical bistability of the single frequency scattering problem, exhibited by these systems.

(a) Symmetric systems. A simple case of interest is that of two different frequency modes for which $a_1 = a_2$, $b_1 = b_2$, $c_1 = c_2$, $d_1 = d_2$. The system of two equations in this case is symmetric in its parametrization. This parametrization is a reasonable consideration for a model of two guided modes with closely spaced frequencies such as would be found in the same pass band of a photonic crystal waveguide or two closely space modes in a metamaterial. In addition, in both systems the guided mode dispersion relations should be relatively flat (i.e., approximately dispersionless), consistent with our assumptions in both systems of weak couplings between sites. In most calculations of current interest for applications of the band structures of photonic crystals and the dynamics of metamaterials, frequency independent dielectric and coupling properties of the system are assumed [1–5]. The proposed assumptions then are not inconsistent with current practice.

For this case there is a set of solutions of Eqs. (19) with the property $x = y$. Under these conditions, following the discussions of the polynomial forms in Eqs. (20), the system exhibits a simultaneous unique real solution of both equations of the system when

$$D_1 = D_2 = \frac{1}{27}\left[\frac{b_1}{a_1 + c_1}\right]^3 + \frac{1}{4}\left[\frac{d_1}{a_1 + c_1}\right]^2 > 0. \tag{21}$$

From Eq. (21) the unique solutions are in the regions:

(a) for $b_1 > 0$

$$a_1 + c_1 < -\frac{4}{27}\frac{b_1^3}{d_1^2} \quad \text{or} \quad a_1 + c_1 > 0 \tag{22a}$$

and

(a) for $b_1 < 0$

$$a_1 + c_1 > -\frac{4}{27}\frac{b_1^3}{d_1^2} \quad \text{or} \quad a_1 + c_1 < 0. \tag{22b}$$

Note that for the case in Eq. (22a) the region of multiple solutions is expected in the region $a_1 + c_1 < 0$ and for the case in Eq. (22b) the region of multiple solutions is expected in the region $a_1 + c_1 > 0$. This is seen in the plots and tables discussed later.

In Table I the conditions in Eqs. (22) for the regions in which single valued solutions exist are evaluated for the photonic crystal and metamaterials cases. For the photonic crystal system the conditions of single valued solutions provide limitations on the Kerr parameters of the system through the couplings $\gamma_{ii} = \lambda_{ii}t_i^2$ and $\gamma_{ij} = \lambda_{ij}t_j^2$, where $i = 1, 2$. Similarly, for the metamaterial the conditions are written in terms of mutual inductive and dielectric parameters through the coupling parameters $\gamma_{ii} = \frac{3\alpha}{\varepsilon_l^i}r_{ii}t_i^2$ and $\gamma_{ij} = \frac{2\alpha}{\varepsilon_l^i}r_{ij}t_j^2$, where $i = 1, 2$. As will be discussed in detail later, multiple solutions exist in regions of positive or negative $\gamma_{ij} + \gamma_{ji}$ depending on the parameters characterizing the dispersion relation of the linear waveguide and the Kerr media. The results in Table I can also be used for a comparison of the multiple mode solutions of the two frequency problem with the optical bistability of a single frequency guided mode in the waveguide channel. This follows as the solutions in Table I for $\gamma_{ij} = \gamma_{ji} = 0$ revert to the optical bistability conditions of the system with a single frequency mode in the waveguide channel.

In addition to the $x = y$ solutions, there are nonsymmetric solutions to the systems in Eqs. (18) and (19) for which $x \neq y$. This is a type of symmetry breaking solution arising

TABLE II. The solution for the system in Eq. (25) for the transmission coefficients.

System	Impurity site fields $i, j = 1, 2$	Transmission of modes $i, j = 1, 2$
In-channel photonic crystal	$\tilde{S}_i = \frac{1}{2}\frac{g_l^i}{g^i} \pm \frac{1}{2}\left[\left(\frac{g_l^i}{g^i}\right)^2 - \frac{4}{\gamma}\right]^{1/2}$	$T_i = \frac{4\sin^2 k_i}{4\sin^2 k_i + \left(\frac{\tilde{S}_i - 1}{g_l^i \beta_i}\right)^2}$
	$\tilde{S}_j = \frac{1}{2}\frac{g_l^j}{g^j} \mp \frac{1}{2}\left[\left(\frac{g_l^j}{g^j}\right)^2 - \frac{4}{\gamma}\right]^{1/2}$	$T_j = \frac{4\sin^2 k_j}{4\sin^2 k_j + \left(\frac{\tilde{S}_j - 1}{g_l^j \beta_j}\right)^2}$
Off-channel photonic crystal	$\tilde{S}_i = \frac{1}{2}\frac{g_l^i \beta_i}{1 - g^i \alpha_i} \pm \frac{1}{2}\left\{\left(\frac{g_l^i \beta_i}{1 - g^i \alpha_i}\right)^2 - \frac{4}{\gamma}\left(1 - \frac{g_l^i}{g^i}\left[1 + 2\frac{\beta_i}{\alpha_i}\cos k_i\right]\right)\right\}^{1/2}$	$T_i = \frac{4\sin^2 k_i}{4\sin^2 k_i + \left(\frac{\tilde{S}_i - g_l^i \beta_i}{g_l^i \alpha_i}\right)^2}$
	$\tilde{S}_j = \frac{1}{2}\frac{g_l^j \beta_j}{1 - g^j \alpha_j} \mp \frac{1}{2}\left\{\left(\frac{g_l^j \beta_j}{1 - g^j \alpha_j}\right)^2 - \frac{4}{\gamma}\left(1 - \frac{g_l^i}{g^i}\left[1 + 2\frac{\beta_i}{\alpha_i}\cos k_i\right]\right)\right\}^{1/2}$	$T_j = \frac{4\sin^2 k_j}{4\sin^2 k_j + \left(\frac{\tilde{S}_j - g_l^j \beta_j}{g_l^j \alpha_j}\right)^2}$
Off-channel metamaterial	$\tilde{S}_i = \frac{1}{2}\frac{\omega_l^2 \lambda'_i}{1 - \omega_i^2} \pm \frac{1}{2}\left[\left(\frac{\omega_l^2 \lambda'_i}{1 - \omega_i^2}\right)^2 - 4\frac{\omega_l^2 - 1}{\gamma}\right]^{1/2}$	$T_i = \frac{4\sin^2 k_i}{4\sin^2 k_i + \left(\frac{\lambda'_i}{\lambda_i}\tilde{S}_i\right)^2}$
	$\tilde{S}_j = \frac{1}{2}\frac{\omega_j^2 \lambda'_j}{1 - \omega_j^2} \mp \frac{1}{2}\left[\left(\frac{\omega_j^2 \lambda'_j}{1 - \omega_j^2}\right)^2 - 4\frac{\omega_j^2 - 1}{\gamma}\right]^{1/2}$	$T_j = \frac{4\sin^2 k_j}{4\sin^2 k_j + \left(\frac{\lambda'_j}{\lambda_j}\tilde{S}_j\right)^2}$

from the multiplicity of unknowns and the nonlinearity of the equations. The resulting solutions do not have a counterpart in the single frequency guided mode problem and are only present in multiple mode problems. The additional solutions are given by

$$x = \frac{1}{2}\frac{d}{(c-a)r} + \frac{1}{2}\left[\frac{d^2}{(c-a)^2 r^2} - 4r\right]^{1/2}, \tag{23a}$$

$$y = \frac{1}{2}\frac{d}{(c-a)r} - \frac{1}{2}\left[\frac{d^2}{(c-a)^2 r^2} - 4r\right]^{1/2}, \tag{23b}$$

where $a_1 = a_2 = a$, $b_1 = b_2 = b$, $c_1 = c_2 = c$, $d_1 = d_2 = d$, and r is a real root of the cubic polynomial

$$(a + c)\, r^3 - b r^2 - \frac{a d^2}{(c-a)^2} = 0. \tag{23c}$$

[Notice that Eqs. (23) are not defined for the case that $a = c$, and the additional $x \neq y$ solutions do not exist in this limit.] Only a single real solution for r is needed to yield the additional $x \neq y$ solutions to the system of equations. However, Eq. (23c) may have multiple real solutions for r, and these would add to the multiplicity of $x \neq y$ solutions.

A limit of Eqs. (23) that is of general interest for systems with weak nonlinear Kerr coupling parameters is that for which $a,c \ll b,d$. In these systems a,c parametrize the Kerr nonlinear terms and are typically small compared to b,d characterizing the linear properties of the waveguide and impurity. From Eq. (23c) we find for this case that

$$r \approx \sqrt{-\frac{a d^2}{b(c-a)^2}}, \tag{24}$$

and Eqs. (23a) and (23b) with Eq. (24) are valid provided $c \neq a \neq 0$.

An exactly solvable case of the $x \neq y$ system is that for which $c \neq a = 0$ in Eq. (23c). For these systems the $x = y$ solutions of Table I and the $x \neq y$ solutions are both given in closed analytic forms. In this limit

$$r = \frac{b}{c}, \tag{25}$$

where the $x \neq y$ solutions are obtained from Eqs. (23a) and (23b). The results for the transmission coefficients of the $x \neq y$ solutions for these systems are listed in Table II. They will be discussed later.

(b) Asymmetric systems. An additional exactly solvable and experimentally realizable case of interest is that in which one of the equations is not coupled to the other by the nonlinear interaction. This is the case of an asymmetric system in which one frequency mode of the system has a strong interaction with the other mode and a strong self-interaction, but the other mode only has a strong self-interaction. Such interactions can be arranged because the coupling parameters of the nonlinearity (i.e., the parameters $\gamma_{ii} = \lambda_{ii} t_i^2$, $\gamma_{ij} = \lambda_{ij} t_j^2$ in the photonic crystal system and $\gamma_{ii} = \frac{3\alpha}{\varepsilon_l^i} r_{ii} t_i^2$, $\gamma_{ij} = \frac{2\alpha}{\varepsilon_l^i} r_{ij} t_j^2$ in the metamaterial) are related to the intensity of the transmitted waves. As an example, consider a system in which the intensity of one frequency mode is much less than that of the other, i.e., $t_1 \ll t_2$. In this configuration the t_2 system tends to have a smaller (negligible) interaction with the t_1 system than with itself.

For this case the general form of the equations of the system is approximated by

$$a_1 x^3 + (b_1 + c_1 y^2) x - d_1 = 0, \tag{26a}$$

$$a_2 y^3 + b_2 y - d_2 = 0. \tag{26b}$$

In terms of the parameters of the photonic crystal, Eqs. (26) are obtained if $c_2 = \gamma_{21} = \lambda_{21} t_1^2 \ll c_1 = \gamma_{12} = \lambda_{12} t_2^2$, $a_1 = \gamma_{11} = \lambda_{11} t_1^2$. Likewise for the metamaterial $c_2 = \gamma_{21} = \frac{2\alpha}{\varepsilon_l^2} r_{21} t_1^2 \ll c_1 = \gamma_{12} = \frac{2\alpha}{\varepsilon_l^1} r_{12} t_2^2$, $c_1 = \gamma_{11} = \frac{3\alpha}{\varepsilon_l^1} r_{11} t_1^2$ is required for this limit.

From Eq. (20) the condition for Eq. (26b) to have a single valued solution is given by

$$D_2 = \frac{1}{27}\left(\frac{b_2}{a_2}\right)^3 + \frac{1}{4}\left(\frac{d_2}{a_2}\right)^2 > 0 \tag{27a}$$

and the condition for Eq. (26a) to have a single valued solution is given by

$$D_1 = \frac{1}{27}\left(\frac{b_1 + c_1 y^2}{a_1}\right)^3 + \frac{1}{4}\left(\frac{d_1}{a_1}\right)^2 > 0. \tag{27b}$$

A unique solution of the system is obtained provided both of these inequalities are simultaneously satisfied. An example of this system and the novelty of its multiple solutions will be considered later.

We now turn to a presentation and discussion of plots illustrating the above behaviors in a number of systems.

IV. RESULTS

In this section discussions are presented of typical behaviors found for guided modes at two different frequencies interacting with Kerr nonlinear impurities. A focus is on multiple solutions of the transmission coefficients in the two mode problem and how the multiple solution effects observed differ from the optical bistability properties found in the single guided mode problem. The equations given in Sec. II are completely general for the waveguide impurity problem for guided modes at two different frequencies but are restricted here to cases of modes with closely spaced frequencies. In addition, it is assumed that the dispersion relations of the modes are relatively flat. These restrictions facilitate the study of the possible behaviors in the systems while offering an indication of the qualitative behaviors expected in more general cases.

A. Photonic crystals

For two guided modes with closely spaced frequencies, the frequency dependent parameters characterizing the dielectric properties of the waveguide should be approximately the same. Under this reasonable assumption the ratios of the linear parts of the dielectric constants satisfy $\frac{g_l^1}{g^1} \approx \frac{g_l^2}{g^2}$, and the Kerr parameters satisfy $\lambda_{ii} \approx \lambda_{jj}$ and $\lambda_{ij} \approx \lambda_{ji}$, for $i, j = 1,2$, where $i \neq j$. In addition, each of the two close frequencies should have a similar interaction with the system so that it is expected that λ_{ii} and λ_{ij} are the same sign, and the ratios of the on-site and nearest neighbor couplings are relatively frequency independent with $\frac{\beta_1}{\alpha_1} \approx \frac{\beta_2}{\alpha_2}$. As has been shown in previous work on the properties of photonic crystal waveguides, the ratio $\frac{\beta_1}{\alpha_1} \approx \frac{\beta_2}{\alpha_2}$ measures the spatial decay rate of electromagnetic radiation at stop band frequencies in the bulk photonic crystal so that by adjusting the separation between neighboring sites chosen to form the waveguide channel $|\frac{\beta_1}{\alpha_1}| \ll 1$ can be assured [47]. This last condition guarantees that the guided mode dispersion relations are flat and our nearest neighbor coupling model is correct. Such examples of the choice of waveguide couplings have been presented in our previous work on photonic crystal waveguides [22–24,29,30,34,35,47,54].

First consider the system in Fig. 1(a) for the in-channel impurity. It is convenient to study the transmission coefficients of this system in terms of the parameters $\gamma_{ii} = \lambda_{ii} t_i^2$, $\gamma_{ij} = \lambda_{ij} t_j^2$. In this parametrization, for fixed values of the Kerr parameters characterizing the nonlinearity, the multiple solution properties are represented in terms of the variation of the intensities of the two transmitted waves. As a further simplification in the presentation, only the cases for which $\gamma_{ii} = \gamma_{jj} = \gamma_{ij} = \gamma_{ji} = \gamma$ and for which $\gamma_{ii} = \gamma_{jj} = 0$, $\gamma_{ij} = \gamma_{ji} = \gamma$ are treated. These represent limiting forms of the system and provide representative behaviors of the new physical features in the two mode systems. The first case displays the limit in which the system only has symmetric solutions. The second case is an example of a general solution composed of both symmetric and nonsymmetric components and, in addition, has a simple closed form expression for the transmission coefficients.

Figure 2 displays plots of the transmission coefficient versus γ for the two cases of $\gamma_{ii} = \gamma_{jj}$ and $\gamma_{ij} = \gamma_{ji}$. In the plots the ratio of the nearest neighbor to on-site couplings for our theory of weakly coupled waveguide systems is taken as $\frac{\beta_1}{\alpha_1} = \frac{\beta_2}{\alpha_2} = 0.1$. In general, the qualitative and quantitative behaviors in Fig. 2 are found to be weakly dependent on these ratios, and the values of the ratios are typical to our earlier discussions [5,6,22–24,29,30,34–36,41,47,54] of photonic crystal waveguides. The ratios $\frac{g_l^i}{g^i}$ involving the linear and nonlinear channel sites are taken to be $\frac{g_l^1}{g^1} = \frac{g_l^2}{g^2} = 3$. This is a reasonable choice for these ratios, and provides a nice illustration of the qualitative behavior found in typical systems. For the plot $k_1 = k_2 = 1.0$ is located roughly midway between the center and edge of the waveguide Brillouin zone.

In Fig. 2(a) the transmission coefficients as a function of γ for the two guide modes of the purely symmetric $\gamma_{ii} = \gamma_{jj} = \gamma_{ij} = \gamma_{ji} = \gamma$ case are presented. The transmission results are the same for each of the two modes. For each mode, the system exhibits multiple solutions in the region $-\frac{2}{243} < \gamma < 0$, and as seen from Table I only systems with negative Kerr parameters have a region of multiple solutions. In the region of multiple solutions, for each of the modes, three solutions for the transmission coefficients are found. Two solutions have small values for the transmission coefficient that decrease to zero as negative γ approaches zero. The third solution rises rapidly to a transmission coefficient less than unity as negative γ approaches zero. The nature of the multiple solutions is understood by changing γ. Beginning in the linear limit of the system at $\gamma = 0$, as γ is decreased into the region $-\frac{2}{243} < \gamma < 0$ the transmission coefficients of the system travel along the upper branch in Fig. 2(a) until they fall off at $\gamma = -\frac{2}{243}$. The coefficients then follow with decreasing γ the single branch of transmission coefficients in the region $\gamma < -\frac{2}{243}$. Upon reversing this trajectory, the system begins on the single lower branch at $\gamma < -\frac{2}{243}$ and moves on the lower branch of the transmission coefficient curve until at $\gamma = 0$ it switches to the limit of the linear system on the upper branch. In the region of multiple solutions a form of optical bistability is then exhibited by each of the two frequencies. The behavior of each of the two modes is reminiscent of the optical bistability of the single frequency system observed in the plot found in Fig. 3 of Ref. [47]. In Fig. 3 of Ref. [47] as the intensity of the single mode is increased and then decreased a similar switching is found between three branches of the system solutions. The region of bistability of the two mode system, however, is found to be different from that of the single frequency system. The multiple solution interval of the two frequency system is half the size in γ of that of the single modes system.

In Fig. 2(b) the transmission coefficients for the $\gamma_{ii} = \gamma_{jj} = 0$, $\gamma_{ij} = \gamma_{ji} = \gamma$ case are shown as a function of γ.

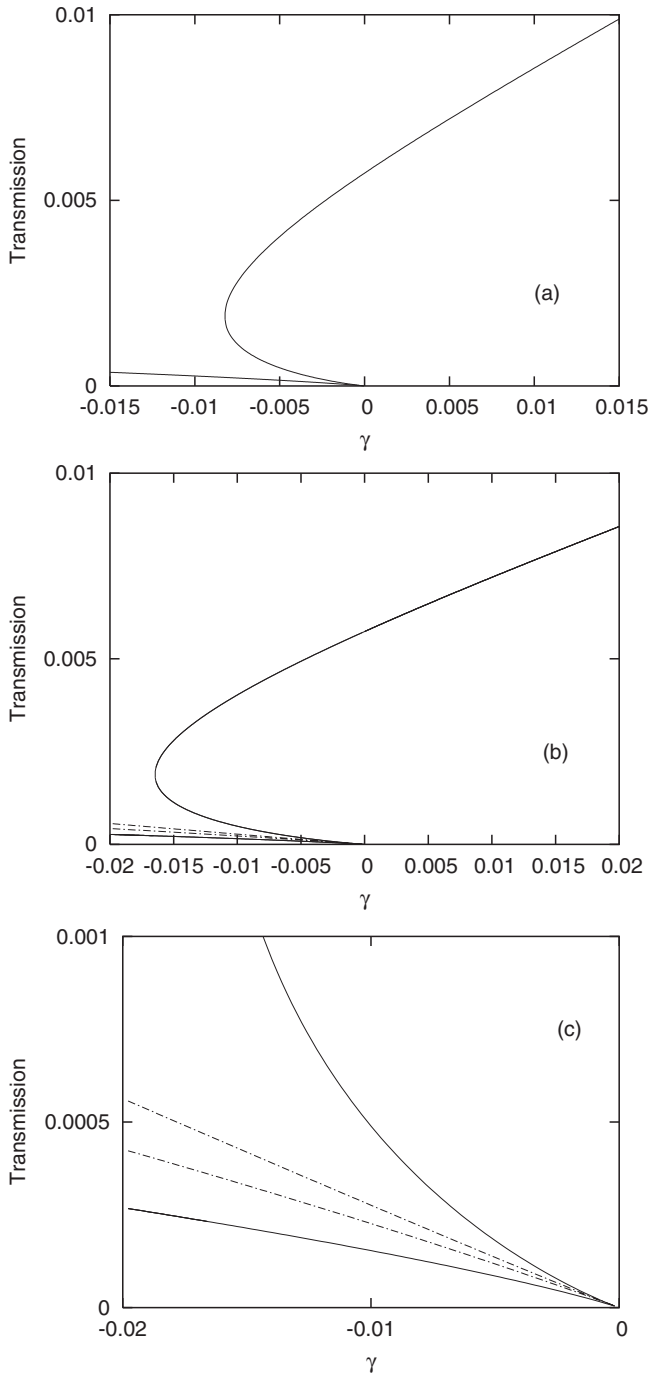

FIG. 2. Plots of photonic crystal results for an in-channel impurity as in Fig. 1(a) for: (a) Plot of the transmission coefficient versus γ for $\gamma_{ii} = \gamma_{jj} = \gamma_{ij} = \gamma_{ji} = \gamma$. The region of multiple transmission coefficient solutions is $-\frac{2}{243} < \gamma < 0$. (b) Plot of the transmission coefficient versus γ for the case $\gamma_{ii} = \gamma_{jj} = 0$ and $\gamma_{ij} = \gamma_{ji} = \gamma$. (c) An amplified portion of the plot in (b). The region of multiple transmission coefficient solutions is $-\frac{4}{243} < \gamma < 0$. For the plots $\frac{\beta_1}{\alpha_1} = \frac{\beta_2}{\alpha_2} = 0.1$, $k_1 = k_2 = 1.0$, and $\frac{g_l^1}{g^1} = \frac{g_l^2}{g^2} = 3$. In the figures the solid lines are for the symmetric solutions and the dashed lines are for the nonsymmetric solutions.

In this limit the system has both symmetric (solid lines) and nonsymmetric (dashed lines) transmission coefficient solutions. Figure 2(b) displays a region of symmetric multiple transmission coefficients for $-\frac{4}{243} < \gamma < 0$. For the symmetric solutions two of the transmission coefficients go to zero as negative $\gamma \to 0$ while the third solution rises rapidly to a transmission coefficient less than unity as negative $\gamma \to 0$. As with Fig. 2(a) the plot of the symmetric transmission coefficients is a hysteresis type of curve. In addition, a region of nonsymmetric transmission coefficient solutions is found to include all of $\gamma < 0$, but for $\gamma > 0$ nonsymmetric solutions do not exist. To facilitate the reader the region of the plot containing nonsymmetric solutions has been amplified and presented in Fig. 2(c). For $\gamma < 0$ the nonsymmetric solutions exhibit two transmission coefficients that are split between the frequencies so if one is fixed upon by the frequency labeled 1 the other is for the frequency labeled 2. For $\gamma \to 0$ the antisymmetric transmission coefficients have the limiting forms for the two modes labeled $i = 1,2$,

$$T_i^{\pm} \to -\frac{4\gamma\left(g_l^i\beta_i\right)^2\sin^2 k_i}{1 \mp 2\sqrt{-\gamma}\left(1 - \frac{1}{2}\frac{g_l^i}{g^i}\right)} \tag{28a}$$

where for the $\pm$ transmission coefficients are split between the two modes. These are to be compared to the degenerate lowest branches of the symmetric solutions given by

$$T_i^{\pm} \to -\frac{4\gamma\left(g_l^i\beta_i\right)^2\sin^2 k_i}{1 \mp \left(\frac{g_l^i}{g_i} + 2\right)\sqrt{-\gamma}}, \tag{28b}$$

where both modes take the same $\pm$ transmission coefficient.

The nonsymmetric solutions are seen to exhibit a symmetry breaking between the transmission coefficients of the two guided modes similar to that found in Jahn-Teller systems. As with the Jahn-Teller effect the symmetry breaking is a feature arising from the nonlinearity introduced into the system by the Kerr nonlinearity of the impurity site media.

Another interesting type of behavior for two frequency modes interacting with the Kerr impurity is the case of asymmetric couplings between the two frequencies. This differs from the results discussed earlier which are for symmetric couplings between the two modes. Asymmetrically coupled modes exhibit more complex forms of multiple transmission solutions. In Fig. 3 results are presented for an asymmetric system in which $\gamma_{ii} = \gamma_{jj} = \gamma_{ij} = \gamma$ and $\gamma_{ji} = 0$. For these couplings the nonlinear interaction of one frequency mode is only with itself while the nonlinear interactions of the other frequency mode involve a self-interaction along with an interaction with the other frequency mode in the system. Figure 3(a) presents the transmission coefficients as functions of γ for the frequency with a self-interaction and an interaction with the other frequency in the system, while Fig. 3(b) presents results for the frequency mode with only a self-interaction. The results in Fig. 3(b) for the mode with only a self-interaction display a standard optically bistable transmission. This is due to the lack of influence on this mode from the other mode in the system. The curves in Fig. 3(b) are labeled 1, 2, 3 for the different branches of the optical bistable solutions, and all three curves coexist in the region $-\frac{4}{243} < \gamma < 0$ of optical bistability. The results in Fig. 3(a) display an additional multiplicity of transmissions arising from its self-interaction and the additional interaction with the other

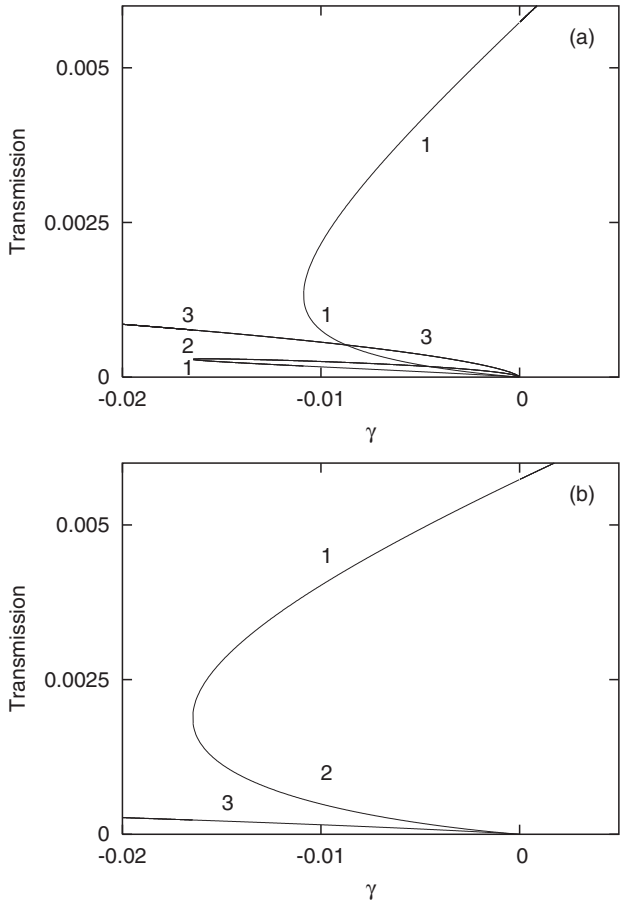

FIG. 3. In-channel photonic crystal results for: (a) Plot of the transmission coefficient versus γ for the frequency with both self-interaction and interaction with the other frequency mode. The region of multiple transmission coefficient solutions is $-\frac{4}{243} < \gamma < 0$. (b) Plot of the transmission coefficient versus γ for the frequency with only a self-interaction. In these illustrative plots the case in which $\frac{\beta_1}{\alpha_1} = \frac{\beta_2}{\alpha_2} = 0.1$, $k_1 = k_2 = 1.0$, and $\frac{g_l^1}{g^1} = \frac{g_l^2}{g^2} = 3$ is considered. The numbering of the curves pairs the solution sets of the transmission coefficient of the system and is explained in the text.

frequency mode in the system. This gives a more complex behavior than that observed in optically bistable systems. Specifically, the transmission coefficients have a region of five different solutions rather than the three solutions typical of optical bistability. The curves in Fig. 3(a) are labeled 1, 2, 3 to correlate them with the curves labeled 1, 2, 3 in Fig. 3(b). The solution labeled $i = 1, 2, 3$ in Fig. 3(a) is paired with the solutions labeled $i = 1,2,3$ in Fig. 3(b) to form pairs (i,i) of multiple solutions for the two mode system. Considering all of the modal solutions in the system for each of the two frequencies, it is found that the absence of multiple solutions is only on the intersections of the two regions defined separately from Eq. (20b) for the two frequencies. Consequently, the region of multiple transmission coefficient solutions, from Eqs. (11) and (27), is $-\frac{4}{243} < \gamma < 0$.

The transmission coefficients with the same numerical labels presented in Figs. 3(a) and 3(b) are paired together to form the possible observed transmission states of the total system. These solutions can be understood as follows: Starting at the $\gamma = 0$ linear limit of the system, both frequencies have transmission coefficients $T_i \approx 0.0057$ for $i = 1,2$, which are on curves labeled 1 in their respective plots. As $|t|^2$ is increased and the system becomes more nonlinear, the transmission coefficients of the modes move into regions of positive or negative γ depending on the signs of the Kerr couplings. For increasing positive γ there are only a set of unique transmission coefficient solutions, and this case is not of interest. For increasing negative γ the transmission coefficients of the two modes move along the curves labeled 1 upon which they started. Eventually, near $\gamma = -0.011$ the mode in Fig. 3(a) falls off its curve labeled 1. It jumps to another curve labeled 1 in Fig. 3(a) which is another solution paired with the solution labeled 1 in Fig. 3(b). The jump in Fig. 3(a) is to the multiple solution curve labeled 1 with the lowest transmission coefficients. After this jump, both modes continue to move on their curves labeled 1 until $\gamma = -\frac{4}{243}$. At this point both modes jump to the transmission coefficient curves labeled 3 as γ becomes increasingly more negative. The system is no longer in a region of multiple solutions. Trying to return to the linear limit, both modes begin on the far left of the plot along the curves labeled 3 in the region without multiple solutions. As both modes approach the origin at $\gamma \approx 0$ they both jump to the curves labeled 1 containing the linear limit $T_i \approx 0.0057$ for $i = 1, 2$.

Next consider the system in Fig. 1(b) for the off-channel impurity. Under the restriction that $\gamma_{ii} = \gamma_{jj}$ and $\gamma_{ij} = \gamma_{ji}$ a solution of symmetric form is found which exhibits significantly different physics from that of the in-channel impurity problem. While in the case of the in-channel problem multiple solutions are only present in the case of negative Kerr parameters, in the off-channel case multiple solutions are found for both positive and negative Kerr parameters. From Table I a region of multiple solutions occurs for negative Kerr interactions when

$$1 - \frac{g_l^i}{g^i}\left[1 + 2\frac{\beta_i}{\alpha_i}\cos k_i\right] > 0 \tag{29a}$$

and a region of multiple solutions occurs for positive Kerr interactions when

$$1 - \frac{g_l^i}{g^i}\left[1 + 2\frac{\beta_i}{\alpha_i}\cos k_i\right] < 0. \tag{29b}$$

In both cases the conditions determining the signs of the Kerr interactions at which multiple solutions occur are expressed in terms of the dielectric properties of the waveguide channel, the dielectric properties of the impurity site, the couplings between the fields along the waveguide, and the wave vector of the guided modes incident on the impurity. For the case that $|\gamma| \ll 1$ that is of interest here, the nonsymmetric solutions in Table II also exhibit a region of multiple solutions for negative Kerr interaction when $1 - \frac{g_l^i}{g^i}[1 + 2\frac{\beta_i}{\alpha_i}\cos k_i] > 0$ and a region of multiple solutions for positive Kerr interactions when $1 - \frac{g_l^i}{g^i}[1 + 2\frac{\beta_i}{\alpha_i}\cos k_i] < 0$. An illustration of some of these regions over a range of γ's is now given for specific examples of the transmission coefficient. To keep the discussions brief only the $\gamma_{ii} = \gamma_{jj} = \gamma_{ij} = \gamma_{ji} = \gamma$ case is treated, showing regions of the Kerr parameters for which multiple solutions are obtained.

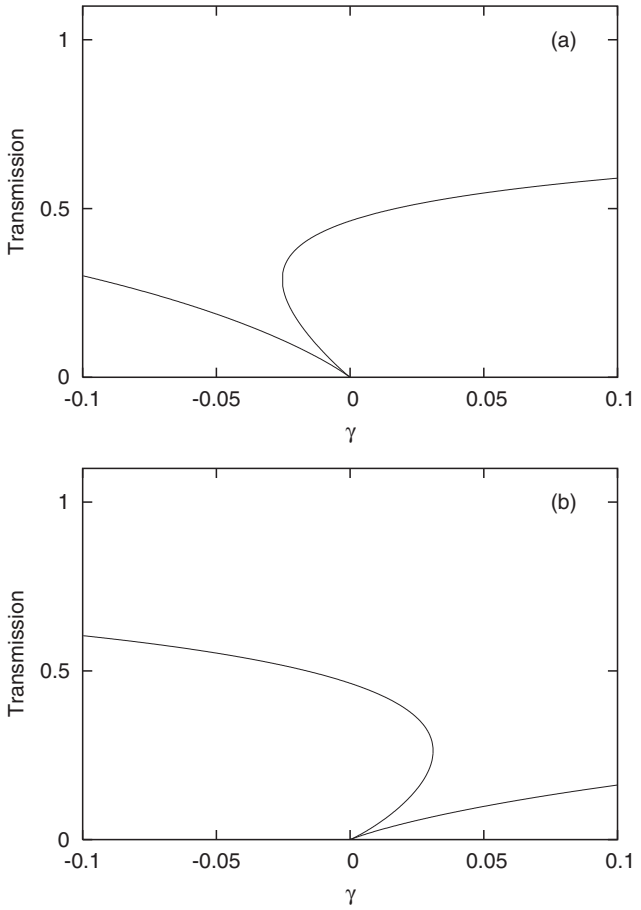

FIG. 4. Off-channel photonic crystals plot of the transmission coefficient versus γ for the case in which: (a) $\gamma_{ii} = \gamma_{jj} = \gamma_{ij} = \gamma_{ji} = \gamma$ with a region of multiple transmission coefficient $-0.025 < \gamma < 0$. (b) $\gamma_{ii} = \gamma_{jj} = \gamma_{ij} = \gamma_{ji} = \gamma$ with a region of multiple transmission coefficient $0.031 > \gamma > 0$. For the illustrative plots in (a) $\frac{\beta_1}{\alpha_1} = \frac{\beta_2}{\alpha_2} = 0.0468$, $k_1 = k_2 = 2.9$, and $\frac{g_l^1}{g^1} = \frac{g_l^2}{g^2} = 1$. For the plots in (b) $\frac{\beta_1}{\alpha_1} = \frac{\beta_2}{\alpha_2} = 0.0572$, $k_1 = k_2 = 0.242$, and $\frac{g_l^1}{g^1} = \frac{g_l^2}{g^2} = 1$.

In Fig. 4 plots of the transmission coefficient versus γ are presented for $\gamma_{ii} = \gamma_{jj} = \gamma_{ij} = \gamma_{ji} = \gamma$. As noted earlier, in this case the complication of a nonsymmetric solution of the type in Table II is not present. For these examples we will also assume the condition $\frac{g_l^1}{g^1} = \frac{g_l^2}{g^2} = 1$ so that the dielectric contrast between the waveguide and the impurity is determined by the nonlinear part of the Kerr dielectric constant. This simplifies the conditions in Eqs. (29) for the sign of the Kerr parameter so that it now depends on that of the ratio $-2\frac{\cos k_i}{\alpha_i/\beta_i}$. It is interesting to see that for a fixed ratio of $\frac{\beta_i}{\alpha_i}$, depending on the choice made for k_i, the system exhibits both multiple solution regions of positive and negative Kerr parameters. The results in Fig. 4(a) are an example of a system with multiple solutions in the region of negative Kerr parameters while the results in Fig. 4(b) are for a system with positive Kerr parameters. In particular, the plots in Fig. 4(a) are made for $\frac{\beta_1}{\alpha_1} = \frac{\beta_2}{\alpha_2} = 0.0468$ and $k_1 = k_2 = 2.9$, while the plots in Fig. 4(b) are made for $\frac{\beta_1}{\alpha_1} = \frac{\beta_2}{\alpha_2} = 0.0572$ and $k_1 = k_2 = 0.242$. For the plot in Fig. 4(a), Eq. (29a) gives $-2\frac{\cos k_i}{\alpha_i/\beta_i} = 0.091$ and the region of multiple solutions occurs for negative Kerr parameters (i.e., $\gamma < 0$). For the plot in Fig. 4(b), Eq. (29b) gives $-2\frac{\cos k_i}{\alpha_i/\beta_i} = -0.111$ and the region of multiple solutions occurs for positive Kerr parameters (i.e., $\gamma < 0$). In both cases the figures illustrate typical behaviors of the symmetric solutions.

B. Metamaterials

In Eqs. (4) and (5) for the metamaterial systems it will be assumed that the two frequencies of the guided modes are close together. As a consequence, it follows that $\frac{\alpha}{\varepsilon_l^i} r_{ii} \approx \frac{\alpha}{\varepsilon_l^j} r_{jj}$ and $\frac{\alpha}{\varepsilon_l^i} r_{ij} \approx \frac{\alpha}{\varepsilon_l^j} r_{ji}$ for $i, j = 1,2$, and the signs of the $\frac{\alpha}{\varepsilon_l^i} r_{ii}$ and $\frac{\alpha}{\varepsilon_l^i} r_{ij}$ are the same. In addition, it is assumed that the mutual inductive couplings are weak so that only nearest neighbor couplings need be considered and these are the same all along the chain. This can be arranged by adjusting the separation between the SRR or the radii of the SRR. In the examples given later the values of the parameters characterizing the nonlinearity and the self- and mutual inductances are taken from earlier works on the SRR model of metamaterials [9,14–16,32,33]. These are known to provide representations of physically realistic systems.

As noted earlier, for two incident frequency modes the in-channel system in Fig. 1(a) displays an absence of multiple transmission coefficient solutions. The Kerr interactions lead to a renormalization of the transmission and reflection properties of the system as field intensities are changed but multiple solutions are not obtained. In addition, in the problem involving a single incident frequency mode there is also an absence of optical bistability for the in-channel case. This is a fundamental difference from the properties of the photonic crystal and the metamaterial systems with off-channel impurities and the photonic crystal with in-channel impurities. These last systems exhibit regions of multiple solutions and regions of optical bistability for problems involving a single incident frequency mode.

The nonlinearity of the off-channel impurity problem in Fig. 1(b) is characterized by the parameters $\gamma_{ii} = 3\frac{\alpha}{\varepsilon_l^{ii}} r_{ii} t_i^2$ and $\gamma_{ij} = 2\frac{\alpha}{\varepsilon_l^{ij}} r_{ij} t_j^2$. Under the restriction that $\gamma_{ii} = \gamma_{jj}$ and $\gamma_{ij} = \gamma_{ji}$ from Table I multiple valued solutions are found in the region of negative $\frac{\alpha}{\varepsilon_l^{ii}}, \frac{\alpha}{\varepsilon_l^{ij}}$ when

$$\left(\omega_l^2 - 1\right) = -2\omega_i^2 \lambda_i \cos k_i > 0 \tag{30a}$$

and in the region of positive $\frac{\alpha}{\varepsilon_l^{ii}}, \frac{\alpha}{\varepsilon_l^{ij}}$ when

$$\left(\omega_l^2 - 1\right) = -2\omega_i^2 \lambda_i \cos k_i < 0. \tag{30b}$$

As in the case of the photonic crystal with an off-channel impurity, depending on the parameters characterizing the linear waveguide channel, multiple solutions occur for either positive or negative Kerr interactions. The theory of the metamaterial in Sec. II A is for weak mutual inductive couplings so that $\omega_i^2 \approx 1$ and the conditions in Eqs. (30) are primarily set by the λ_i and the wave numbers of the incident guided modes. Some specific examples illustrating these conditions are now given.

Figure 5 displays example plots of the transmission coefficient versus γ's. As a simplification in the presentation, the case for which $\gamma_{ii} = \gamma_{jj} = \gamma_{ij} = \gamma_{ji} = \gamma$ (with only symmetric solutions) and for which $\gamma_{ii} = \gamma_{jj} = 0, \gamma_{ij} = \gamma_{ji} = \gamma$

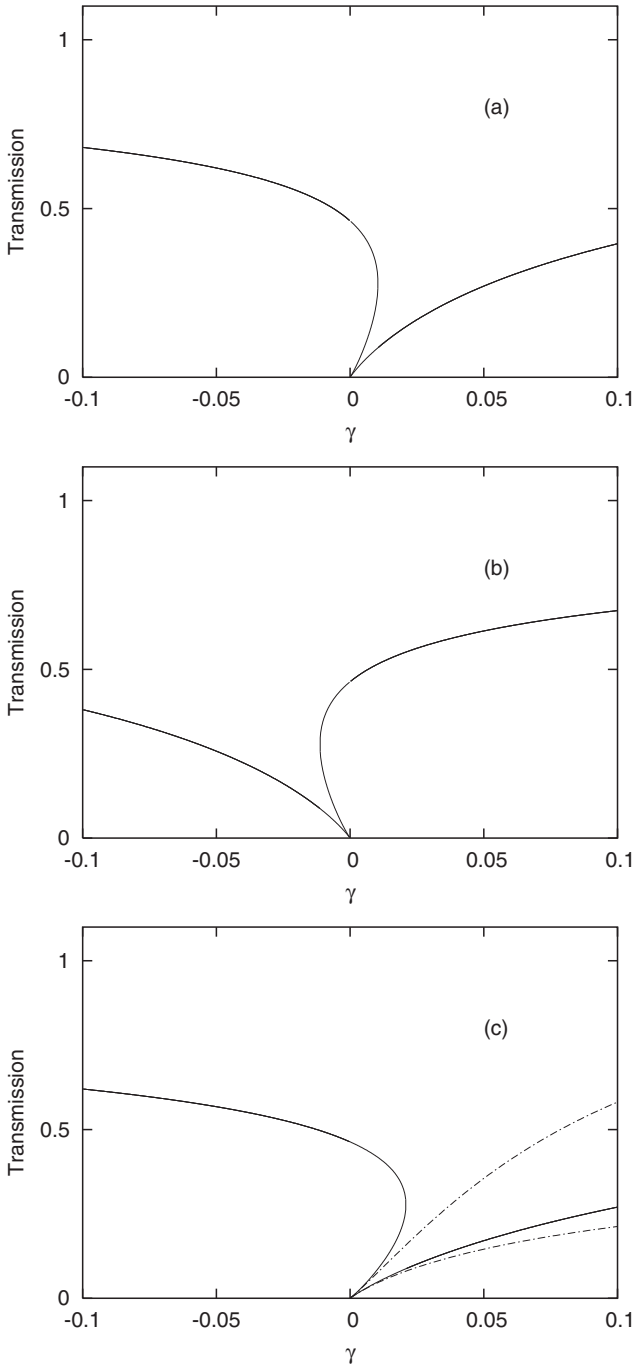

FIG. 5. Plots of off-channel SRR metamaterial transmission coefficient versus γ for: (a) $\gamma_{ii} = \gamma_{jj} = \gamma_{ij} = \gamma_{ji} = \gamma$, $k_1 = k_2 = 2.9$, $\lambda_1 = \lambda_2 = -0.02$, and $\lambda_1' = \lambda_2' = \pm 0.02$. The region of multiple transmission coefficient solutions is $0.0 < \gamma < 0.0104$. (b) $\gamma_{ii} = \gamma_{jj} = \gamma_{ij} = \gamma_{ji} = \gamma, k_1 = k_2 = 2.9, \lambda_1 = \lambda_2 = 0.02$, and $\lambda_1' = \lambda_2' = \pm 0.02$. The region of multiple transmission coefficient solutions is $-0.0113 < \gamma < 0.0$. (c) $\gamma_{ii} = \gamma_{jj} = 0$, $\gamma_{ij} = \gamma_{ji} = \gamma$, $k_1 = k_2 = 2.9$, $\lambda_1 = \lambda_2 = -0.02$, and $\lambda_1' = \lambda_2' = \pm 0.02$. The symmetric transmission solutions are given by the solid lines and the nonsymmetric transmission solutions are given by the dashed lines. The region of multiple transmission coefficient solutions is $0.0 < \gamma < 0.0209$ for the symmetric case and $0.0 < \gamma$ for the nonsymmetric case.

(with both symmetric and nonsymmetric solutions) are treated. In Figs. 5(a) and 5(b) the transmission coefficient of the $\gamma_{ii} = \gamma_{jj} = \gamma_{ij} = \gamma_{ji} = \gamma$ case is shown as a function of γ. The results in Fig. 5(a) are an example of a system in which $\omega_i^2 < 1$ for which the multiple solutions occur for positive nonlinear coupling parameters. The results in Fig. 5(b) are for a system in which $\omega_i^2 > 1$ for which the multiple solutions occur at negative nonlinear coupling parameters. This is unlike the results in Fig. 2 for the in-channel photonic crystal which has multiple solutions only in one quadrant, but similar to the results in Fig. 4 for the off-channel photonic crystal.

In Fig. 5(c) the transmission coefficient of the $\gamma_{ii} = \gamma_{jj} = 0$, $\gamma_{ij} = \gamma_{ji} = \gamma$ case is shown as a function of γ for a $\omega_i^2 < 1$ system. The results are shown for the symmetric solutions (solid lines) and the nonsymmetric solutions (dashed lines) with a region of multiple solutions for positive γ. Similar results are found for $\omega_i^2 > 1$ systems, but in this case the regions of multiple solutions are for negative γ. For the symmetric transmission coefficients a region of multiple transmission coefficients is observed for $0 < \gamma < 0.0209$. In this region the symmetric solution transmission coefficients exhibit two transmission coefficients going to zero as positive $\gamma \to 0$, while the third transmission coefficient rises rapidly to a value less than unity as positive $\gamma \to 0$. As with Figs. 2(a) and 5(a) the plot of the symmetric transmission coefficients is a hysteresis type of curve. In addition, a region of nonsymmetric transmission coefficient solutions is found to include all of $\gamma > 0$, but for $\gamma < 0$ nonsymmetric solutions do not exist. For $\gamma > 0$ the nonsymmetric solutions exhibit two transmission coefficients that are split between the frequencies so if one is fixed upon by the frequency labeled 1 the other is for the frequency labeled 2.

For $\gamma \to 0$ the nonsymmetric transmission coefficients have the limiting forms for the two modes labeled $i = 1,2$,

$$T_i^{\pm} \to 4\left(\frac{\lambda_i}{\lambda'_i}\right)^2 \frac{\gamma}{1-\omega_i^2} \frac{\sin^2 k_i}{1 \mp \frac{\omega_i^2 \lambda'_i}{1-\omega_i^2}\sqrt{\frac{\gamma}{1-\omega_i^2}}}, \tag{31a}$$

where for the $\pm$ transmission coefficients are split between the two modes. These are to be compared to the degenerate lowest branches of the symmetric solutions given by

$$T_i^{\pm} \to 4\left(\frac{\lambda_i}{\lambda'_i}\right)^2 \frac{\gamma}{1-\omega_i^2} \frac{\sin^2 k_i}{1 \mp \frac{\omega_i^2 \lambda'_i}{(\omega_i^2-1)^2}\sqrt{(1-\omega_i^2)\,\gamma}}. \tag{31b}$$

As with the nonsymmetric modes of the photonic crystal, the nonsymmetric solutions of the metamaterial exhibit a lack of symmetry between the transmission coefficients of the two guided modes similar to that found in Jahn-Teller systems.

V. CONCLUSIONS

The multiple solution properties of photonic crystal and SRR waveguides for the propagation of two guided modes at different frequencies in the presence of in- and off-channel Kerr nonlinear dielectric impurities are discussed for systems with weak nearest neighbor couplings [35,47]. The photonic crystal and SRR metamaterial systems are described by nonlinear difference equations in which the interaction of the two guided modes with themselves and each other, generated

by the nonlinearity, is the source of the multiple transmission coefficient solutions [14–16,22–30,32–36]. The two guided modes are found to exhibit more complex multiple solution behaviors in their transmission coefficients than those found in the optical bistability of the systems of single guided modes. This arises from the additional interactions of the two modes with one another.

Both photonic crystals and SRR metamaterials are of interest because they are the focus of current efforts related to technological and device applications. In addition, nonlinearity enters differently in photonic crystal and metamaterial difference equations giving rise to qualitatively differences in their nonlinear behaviors. This allows for an interesting comparison of the qualitative behaviors found between the two systems and between their different types of difference equations. In the photonic crystal model the nonlinearity enters through both on-site and between site couplings [29,30], while the SRR system has nonlinear on-site couplings from the capacitor gaps in the SRR but only linear inductive couplings between the SRRs [14–16]. One consequence of this is that while both photonic crystals and SRRs exhibit multiple solutions in the case of off-channel impurities only photonic crystals exhibit multiple solutions for in-channel impurities.

The regions of multiple solutions come from the solutions of cubic polynomial forms arising in the sets of nonlinear difference equations describing the photonic crystal and SRR systems, and the regions of single and multiple transmission solutions are determined by the solvability conditions of cubic equations [35,47,53]. Analytic forms for the conditions under which multiple transmission coefficient solutions exist are given for the cases of both single and two guided modes traveling in the system. In the presence of two frequencies, single solution regions are determined separately from the intersection of the regions defined by the condition for single valued solutions at each frequency. These regions have then been studied with specific examples of particular solutions within the regions accessible to the systems and for closely spaced frequency modes.

The physics exhibited in these impurity problems is summarized in the following points.

(1) Two different frequency modes propagating in photonic crystals and metamaterials interacting with Kerr nonlinear impurities exhibit additional solutions above those found in the optical bistability of single modes propagating in these systems. This is clearly seen in the increase complexity of the transmission plots of the two mode systems in this paper over that of the optical bistability plots for the single mode photonic crystal given in Fig. 3 of Ref. [47]. These include: (a) For systems with symmetrically coupled difference equations considered in Figs. 2, 4, and 5, new symmetric and nonsymmetric modal solutions introduced in Sec. III C 1 a and presented in Table II. The total number of modal solutions (eight possible modes) is increased over those (three possible modes) found in the regions of optical bistability for a single mode in the system. (b) For the system with asymmetrically coupled difference equations considered in Fig. 3, one mode of the system only has self-interacts while the other mode includes both self-interaction and interaction with the other mode in the system. A total of seven modal solutions were observed in Fig. 3 compared to the three found in the optical bistability of the single mode solutions of Ref. [47].

(2) Precise analytic conditions are given in Table I for the conditions needed to observe multiple solutions in regions of positive and negative Kerr parameters. These are expressed for the photonic crystal systems in terms of the dielectric properties of the Kerr media of the impurity, the dielectric properties and couplings of the linear media of the waveguide, and the wave number of the guided modes. For the metamaterials the conditions are given in terms of the dielectric properties of the Kerr and linear media, the mutual and self-inductance, and the wave number of the guided modes. It is also found that for the photonic crystal system in-channel impurities only exhibit multiple solutions in regions of negative Kerr parameters.

(3) In-channel impurities in metamaterials are found not to exhibit multiple solution behaviors while in-channel impurities in photonic crystals do exhibit multiple solutions. This is due to the difference in the way nonlinearity enters the difference equations of photonic crystals and metamaterials. Unlike photonic crystals, metamaterials do not have nonlinear coupling between neighboring sites. This weakens the effects of the nonlinearity on the systems.

(4) Closed form expressions for the transmission coefficients of all of the systems are listed in the text and in Table II in terms of the dielectric parameters of the systems, the couplings in the difference equations, and the wave numbers of the guided modes. While for the most part these results are for general system parameters we have restricted the parameters studied to a number of cases of technological interests.

It is hoped that the analytic results presented will facilitate an understandings of multiple solutions and their occurrence in photonic crystal and SRR waveguides. The analytic conditions should also help in designing experiments for the observation of the unusual multiple solutions not yet measured and offer a rough guide in design considerations. Many types of systems have nonlinear difference equation formulations including photons, magnons, electrons, and additional novel types of nanosystems [55,56]. These systems should yield to a similar type of analysis to that considered here.

ACKNOWLEDGMENT

A.R.M. would like to thank the Department of Physics at University of California, Riverside, for the use of its library facilities during the course of this work.

[1] K. Sakoda, *Optical Properties of Photonic Crystals* (Springer, Berlin, 2001).

[2] J. D. Joannopoulos, P. R. Vilenueve, and S. Fan, *Photonic Crystals* (Princeton University Press, Princeton, 1995).

[3] J. D. Joannopoulos, P. R. Villeneuve, and S. Fan, Nature (London) **386**, 143 (1995).

[4] P. N. Favennec, *Photonic Crystals: Toward Nanoscale Photonic Devices* (Springer, Berlin, 2005).

[5] A. R. McGurn, in *Nonlinear Phenomena Research Perspectives*, edited by C. W. Wang (Nova Science, New York, 2007), Chap. 8.
[6] A. R. McGurn, Complexity **12**, 18 (2007).
[7] G. Parker and M. Charlton, Phys. World **13**, 29 (2000).
[8] A. R. McGurn, *Survey of Semiconductor Physics*, edited by K. W. Boer (Wiley, New York, 2002), Chap. 33.
[9] N. Engheta and R. W. Ziolkowski, *Metamaterials: Physics and Engineering Explorations* (John Wiley and Sons, Piscataway, NJ, 2006), Vol. 5.
[10] S. A. Ramakrishna, Rep. Prog. Phys. **68**, 449 (2005).
[11] J. B. Pendry, A. J. Holden, D. J. Roberts, and W. J. Stewart, J. Phys.: Condens. Matter **10**, 4785 (1998).
[12] D. R. Smith, W. J. Padilla, D. C. Vier, S. C. Nemat-Nasser, and S. Schultz, Phys. Rev. Lett. **84**, 4184 (2000).
[13] J. B. Pendry, Phys. Rev. Lett. **85**, 3966 (2000).
[14] M. Eleftheriou, N. Lazarides, and G. P. Tsironis, Phys. Rev. E **77**, 036608 (2008).
[15] G. V. Eleftheriades, Mater. Today **12**, 30 (2009).
[16] I. Kourakis, N. Lazarides, and G. P. Tsironis, Phys. Rev. E **75**, 067601 (2007).
[17] M. Lapine, M. Gorkunov, and K. H. Ringhofer, Phys. Rev. E **67**, 065601 (2003).
[18] I. V. Shadrivov, S. K. Morrison, and Y. S. Kivshar, Opt. Express **14**, 9344 (2006).
[19] Y. Tamayama, T. Nakanishi, and M. Kitano, Phys. Rev. B **87**, 195123 (2013).
[20] Y.-S. Lee, *Terahertz Science and Technology* (Springer, Berlin, 2009).
[21] Y. S. Kivshar and G. P. Agrawal, *Optical Solitons* (Academic, Amsterdam, 2003).
[22] A. R. McGurn, Phys. Rev. B **77**, 115105 (2008).
[23] A. R. McGurn, J. Phys.: Condens. Matter **20**, 025202 (2008).
[24] A. R. McGurn, J. Phys.: Condens. Matter **21**, 485302 (2009).
[25] T. Dauxois and M. Peyrard, *Physics of Solitons* (Cambridge University Press, Cambridge, 2006), Chap. 3.
[26] A. J. Sievers and J. B. Page, in *Dynamical Properties of Solids*, edited by G. K. Horton and A. A. Maradudin (North-Holland, Amsterdam, 1995), p. 137.
[27] A. J. Sievers and S. Takeno, Phys. Rev. Lett. **61**, 970 (1988).
[28] A. J. Sievers and S. Takeno, Phys. Rev. B **39**, 3374 (1989).
[29] A. R. McGurn, Phys. Lett. A **251**, 322 (1999).
[30] A. R. McGurn, Phys. Lett. A **260**, 314 (1999).
[31] W. Chen and D. L. Mills, Phys. Rev. Lett. **58**, 160 (1987); W. Chen and A. A. Maradudin, J. Opt. Soc. Am. B **5**, 529 (1988).
[32] P. Giri, K. Choudary, A. S. Gupta, A. K. Bandyopadhyay, and A. R. McGurn, Phys. Rev. B **84**, 155429 (2011).
[33] A. R. McGurn, Phys. Rev. B **88**, 155110 (2013).
[34] A. R. McGurn, J. Phys.: Condens. Matter **16**, S5243 (2004).
[35] A. R. McGurn, Organ. Electron. **8**, 227 (2007).
[36] A. R. McGurn, Adv. OptoElectron. **2007**, 92901 (2007).
[37] E. N. Bulgakov and A. F. Sadreev, Phys. Rev. B **80**, 115308 (2009).
[38] E. N. Bulgakov and A. F. Sadreev, Phys. Rev. B **81**, 115128 (2010).
[39] R. W. Boyd, *Nonlinear Optics*, 2nd ed. (Academic, Amsterdam, 2003).
[40] D. L. Mills, *Nonlinear Optics* (Springer, Berlin, 1998).
[41] A. R. McGurn, Phys. Rev. B **53**, 7059 (1996).
[42] J. B. Pendry, D. Schurig, and D. R. Smith, Science **312**, 1780 (2006).
[43] V. G. Veselago, Sov. Phys. Usp. **10**, 509 (1968).
[44] V. M. Agranovich and Yu. N. Gartstein, Phys. Usp. **49**, 1029 (2006).
[45] U. Leonhardt and T. G. Philbin, Prog. Opt. **53**, 69 (2009).
[46] U. Leonhardt and T. G. Philbin, New J. Phys. **8**, 247 (2006).
[47] A. R. McGurn, Chaos **13**, 754 (2003).
[48] L.-D. Haret, T. Tanabe, E. Kuramochi, and N. Notomi, Opt. Express **17**, 21108 (2009).
[49] F. Zhou, Y. Lui, Z.-Y. Li, and Y. Xia, Opt. Express **18**, 13337 (2010).
[50] D. A. B. Miller, S. Des Smith, and C. T. Seaton, IEEE J. Quantum Electron. **17**, 312 (1981).
[51] M. Soljacic, M. Ibanescu, C. Luo, S. G. Johnson, S. Fan, Y. Fink, and J. D. Joannopoulos, SPIE Proc. **5000**, 200 (2003).
[52] P. Wen, M. Sanchez, M. Grose, and S. Esener, Opt. Express **10**, 1273 (2002).
[53] M. R. Spiegel and J. Lui, *Mathematical Handbook of Formulas and Tables*, 2nd ed. (McGraw-Hill, New York, 1999), p. 10.
[54] A. R. McGurn, Phys. Rev. B **61**, 13235 (2000).
[55] S. P. Shipman and S. Venakides, Nonlinearity **25**, 2473 (2012).
[56] S. P. Shipman, J. Ribbeck, K. H. Smith, and C. Weeks, IEEE Photon. J. **2**, 911 (2010).